Optimization Assisted Load Tracing via Hybrid Ant Colony Algorithm for Deregulated Power System

[1]Z. HAMID[**], [2]I. MUSIRIN[*], M. N. A. RAHIM, N. A. M. KAMARI
[*]Centre for Electrical Power Engineering Studies (CEPES), Faculty of Electrical Engineering,
Universiti Teknologi MARA,
40450 Shah Alam, Selangor,
MALAYSIA
[1]zulcromok086@gmail.com, [2]ismailbm@salam.uitm.edu.my,

Abstract: - The development of electricity tracing theory is to solve the problem concerning fair and non-discriminatory transmission service pricing of a deregulated power system. As the traditional methods such as postage stamp allocation and megawatts-mile methodology neglect the consideration of physical power system constraints, the allocation of service charge is said to be unreliable and rather biasing. At the same time, proportional sharing principle (PSP) based power tracing techniques necessitate for matrix inversion process; in which sometimes cannot be performed due to singularity property of the matrix. As a result, the tracing results are unable to be obtained due to error in mathematical operation. To try a new approach, this paper demonstrates the technique to implement Artificial Intelligence (AI) based optimization for performing load tracing, that is, by means of a new hybrid algorithm; Blended Crossover Continuous Ant Colony Optimization (BX-CACO) with simple and easy formulation steps. Experiment on IEEE 30-bus system together with comparative studies justifies the capability of the proposed technique for real system application.

Key-Words: - BIM, BX-CACO, Load Tracing, Matrix Singularity Property, PSP, TLDF

1 Introduction

In the business concerning transmission service pricing of a deregulated power system, losses charge allocation to consumers has been performed through various approaches; however, it is still in debate among researchers as there are several methods that lack of fairness and free-discrimination when allocating the charge. Traditional methods like postage stamp allocation, megawatts-mile methodology, and contractual path method perform the charge allocation by means of transaction, that is, without taking into account the physical constraints of power system like generation-demand balance and current flow direction [1] – [2]. This results to unsatisfactory service and hence leading to discriminatory business on consumers. Later, another approach known as power tracing has been developed to solve the weakness encountered by the previous discriminatory methods; by adopting the consideration of physical power system constraints into the developed technique. According to [3] – [6], power tracing has significant role for determining generators' share contribution to the line flows, losses, and loads, making transparent charge allocation, assessing congestion in power system, and also behaves like a contributor to establish fair transmission serving pricing.

In a vertically integrated power system, as in Malaysia, performing the electricity tracing is less significant as the information like generator and load participation in line flows and losses cannot contribute to any improvement on system performance. Nevertheless, for a deregulated environment as in European countries, tracing the powers contributed by generators and loads is very important for a transparent charge allocation, that is, each consumer will be able to know how much they will be charged on the associated usage of transmission capacity [7]. In [8] – [9], *proportional sharing principle* (PSP) based power tracing has been proposed, which is called as Topological Generation and Load Distribution Factors (TGLDF). Although it is a pioneer method, there are still disadvantages as it necessitates for matrix inversion (which sometimes cannot be performed if the matrix to be inversed is singular) and also, the power system ought to be treated as lossless, which adds hesitation on the tracing results. A circuit theory based power tracing has been proposed by [10], where the basic Ohm's Law was utilized to obtain the traced complex powers. However, this method still confronts with negative sharing problem and hence unable to provide reliable charge allocation. Other methods that implemented matrix operation for electricity tracing can be explored in [11] – [13].

Alternative approach via optimization technique has been implemented in the research conducted by [14], however, lots of constraints to be considered and burdensome formulation technique have made it less attractive among researchers. Artificial Intelligence (AI) tools have been firstly implemented in [15] – [16] for solving electricity tracing problem. In the researches, Genetic Algorithm (GA) and Artificial Bee Colony (ABC) have been incorporated for providing optimal prediction process by Support Vector Machine (SVM) under the guideline of proportional tree method (PTM).

The well known optimization technique, traditional Ant Colony Optimization (ACO) has been widely implemented to solve various engineering problems due to its fast convergence property and solution optimality. As a matter of fact, traditional ACO was developed by M. Dorigo in 1993 [17] – [18], where he was inspired by the behavior of real ant's foraging from one node to another. Performance of the traditional algorithm was justified in Travelling Salesman Problem (TSP), in which later has put ACO to be the fastest algorithm for optimization. Numerous researches have validated the ability of traditional ACO for optimizing voltage stability of power systems, as reported in [19] – [20]. In addition, traditional ACO has also been incorporated into Fuzzy Inference System (FIS) for providing optimal decision making process as has been proven by [21] – [22]. More experiments concerning the performance of traditional ACO can be explored by the researches conducted in [23] – [25]. Nonetheless, as the traditional algorithm applied discrete probability distribution during solution update process, it is rather unsuitable for the applications related to power system, which is a type of continuous domain problem. To mitigate this weakness, K. Socha [26] has proposed continuous domain ACO (ACO_R) for the purpose of continuous domain optimization by adopting Gaussian normal sampling during solution update. The research proved that ACO_R reflected the best performance in terms of computation speed and solution optimality as compared to other population based algorithms.

This paper presents a new technique for real and reactive power load tracing formulation by means of Blended Crossover Continuous Ant Colony Optimization (BX-CACO); the hybridization between crossover operator of GA and original algorithm of ACO_R. The formulation technique is new, original and has uniqueness in terms of simplicity to be applied. In addition, the proposed algorithm is free from assumption like PSP as well as matrix singularity property, which means that it is suitable to be used in any system condition especially under contingencies for the application in voltage stability improvement.

2 The Concept of Load Tracing

In the field of power tracing, there are two tasks for determining the participation of generators and loads; *generation* and *load tracing*. The process for tracing the power participated or extracted by individual load is called *load tracing*, which is the main topic to be discussed in this paper. The performance of the proposed technique in generation tracing point of view has been validated in [27]. As the Distribution Company (DISCO) is the consumer to be charged on the associated losses and generated power, performing load tracing is a necessary task for a Transmission Company (TRANSCO) in providing reliable charge allocation on consumers. The next subsections describe the concept of load's dominion, followed by involved mathematical relationship in real power load tracing and lastly the compulsory consideration when performing reactive power load tracing.

2.1 Load's Dominion

Load's dominion means that a sole power system consists of a load together with transmission lines used for extracting the output power from the respective generators. Thus, any transmission lines and generators that are not used for extracting the power will not be included in such system. For a clear depiction, consider an IEEE 6-bus power system that has two generators, four loads, and seven transmission lines as in Fig. 1.

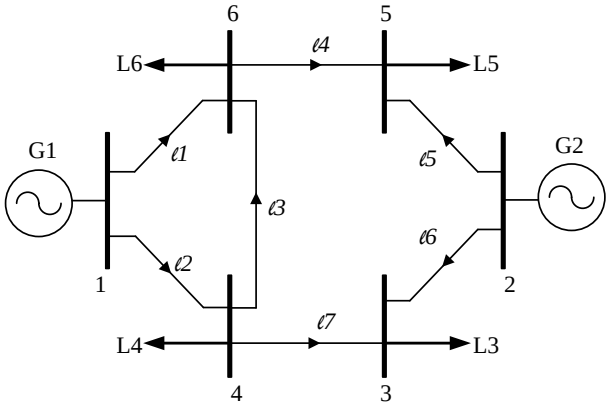

Fig. 1. A simple 6-bus power system with line flow direction.

By considering the line flow direction that entering a load, the following dominions are obtained.

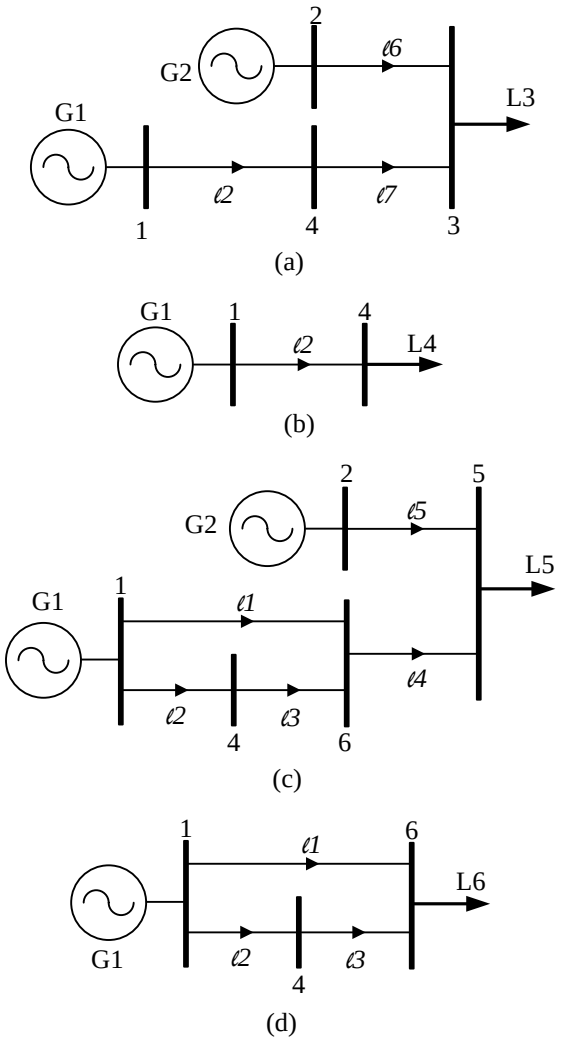

Fig. 2. Dominions of loads: (a) – (d) dominion of load L3, L4, L5, and L6 respectively.

From the figure, it is obvious that load at bus 5 (marked as L5) requires the highest number of transmission lines for extracting the generated power, suggesting that this load becomes the major contributor of losses to the system. Because of that, a TRANSCO should allocate the highest losses charge on this load. On the other hand, load at bus 4 (marked as L4) is said to be the least contributor of losses as the required transmission line is only one and the lowest losses charge is expected from the TRANSCO. Nevertheless, this intuitive expectation is not necessarily reliable because the true method for calculating losses charge is not based on the required number of transmission lines, instead, it is based on the magnitude of contributed losses, that is, the higher the magnitude, the larger the losses charge even if a single line is used.

2.2 Mathematical Relationship

As discussed in the introduction part, formulating a power tracing algorithm requires consideration of physical power system constraints in order that the tracing results are trusty and fair for real application. According to [14], a load with power of P_{Li} participates in line flow and generator's output power by a fraction of x^i, that is:

$$P_{fl}^i = x_{fl}^i . P_{Li} \quad (1)$$

$$P_{gk}^i = x_{gk}^i . P_{Li} \quad (2)$$

Where,

P_{fl}^i : l-th line flow extracted by i-th load
x_{fl}^i : l-th line flow fraction extracted by i-th load
P_{gk}^i : k-th generated power extracted by i-th load
x_{gk}^i : k-th generated power fraction extracted by i-th load

From (1) and (2), it is justified that the percentage of load participation depends mainly on the magnitude of traced powers, not the number of transmission lines. It is essential to note that any unused transmission lines and generators ought to have zero share fraction, for instance, as in Fig. 2(b) load L4 requires only line $\ell 2$ and generator G1 for extracting the power. In virtue of that, the share fractions for other lines and generators must have zero in value (i.e. x_{f1}^4, $x_{f3}^4 - x_{f7}^4$, $x_{g2}^4 = 0$). The line flow of l-th line can be expressed as a summation of individual line flow contributed by each load, as in (3).

$$P_{fl} = P_{fl}^1 + P_{fl}^2 + \ldots + P_{fl}^{nload} \quad (3)$$

Substituting (1) into (3):

$$P_{fl} = x_{fl}^1 . P_{L1} + x_{fl}^2 . P_{L2} + \ldots + x_{fl}^{nload} . P_{L,nload} \quad (4)$$

$$\therefore P_{fl} = \sum_{i=1}^{nload} x_{fl}^i . P_{Li} \quad (5)$$

By using similar mathematical derivation, the following equation is obtained for k-th generated power:

$$\therefore P_{gk} = \sum_{i=1}^{nload} x_{gk}^i . P_{Li} \quad (6)$$

Where, '*nload'* as in (3) to (6) represents the number of loads in the system. For reactive power load tracing, all previous mathematical relationships are applicable, except now the variables '*P*' and '*x*' are replaced by '*Q*' and '*y*' respectively. In addition, because there are alternative elements that are also supplying or consuming reactive power, it is more suitable to replace the terms 'load' and 'generator' with '*reactive sink*' and '*reactive source*' respectively. Mathematical equations for reactive power tracing are represented as follows.

$$Q_{fl}^{i} = y_{fl}^{i} . Q_{Li} \tag{7}$$

$$Q_{sk}^{i} = y_{sk}^{i} . Q_{Li} \tag{8}$$

$$Q_{fl} = \sum_{i=1}^{nsnk} y_{fl}^{i} . Q_{Li} \tag{9}$$

$$Q_{sk} = \sum_{i=1}^{nsnk} y_{sk}^{i} . Q_{Li} \tag{10}$$

Where,

Q_{fl}^{i} : *l*-th line flow extracted by *i*-th reactive sink

y_{fl}^{i} : *l*-th line flow fraction extracted by *i*-th reactive sink

Q_{sk}^{i} : *k*-th reactive source extracted by *i*-th reactive sink

y_{sk}^{i} : *k*-th reactive source fraction extracted by *i*-th reactive sink

Q_{Li} : *i*-th reactive sink power

2.3 Consideration in Reactive Power Tracing

As mentioned in the previous section, the terms reactive sink and reactive source are more suitable as there are also alternative elements that portray one of the characters in reactive power load tracing problem. For instance in the real power tracing viewpoint, a transmission line may be used only for power transportation, however, it can also be a supplier or consumer for reactive power provided that its line flow patterns are considered, especially when performing reactive power tracing. All the alternative elements are discussed below.

i) Shunt elements - There are various types of shunt element which responsible for controlling the reactive power flow such as capacitor bank, FACTS devices (static Var compensator, SVC) as well as capacitive load. All of these reactive power supporters should be modeled as a shunt capacitor installed at a bus as they are also considered as a part of reactive power sources in the system.

ii) Generator source and sink - Apart from shunt elements, the Var support is also provided by generators and synchronous condensers of a power system. Instead of supplying to the system, the generators, however, can also behave as a reactive power sink if it consumes the reactive power like other loads. This implies that the generated reactive power has negative in value.

iii) Line flow pattern of reactive power - Because of its shunt capacitance, a transmission line, besides providing service for power transportation can also become a reactive power source or sink provided that the flow pattern is considered. The recognized flow patterns are illustrated in Fig. 3 (a) – (d).

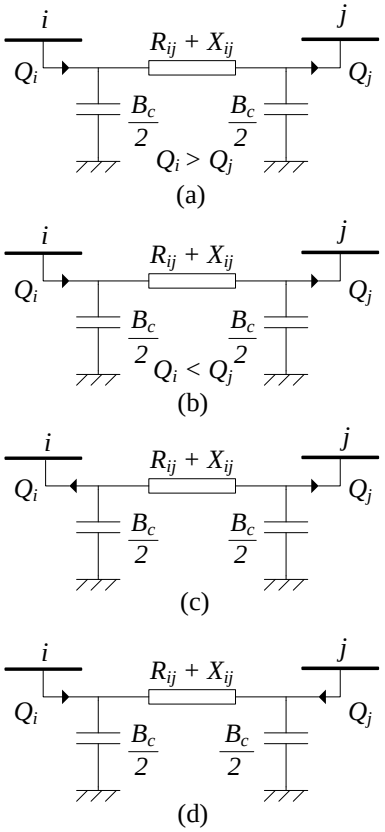

Fig. 3. Line flow pattern: (a) – (d) type 1, 2, 3, and 4 respectively.

From Fig. 3(a), it is seen that the magnitude of line flow at sending end is greater than that of the receiving end, that is, $Q_i > Q_j$. This flow pattern is recognized as type 1. The reactive loss of this line is equivalent to the difference between reactive powers at both ends. Instead of causing the reactive loss, the transmission line can also become a reactive power source provided that the flow patterns as in Fig. 3(b)

and 3(c) are taken into account, which are recognized as type 2 and 3 respectively. This is due to shunt capacitance connected at both ends of the line. In Fig. 3(b), the magnitude of sending end flow is smaller than that of the receiving, implying that there is a source that boosts up the reactive power at the receiving end. In the meantime, Fig. 3(c) depicts the line flows at both ends coming out from the line itself, entailing that it behaves as a reactive power source to the system. For simplicity during coding task, both types are modified to be a single capacitor connected in shunt at bus '*k*' as in Fig. 4(a) with magnitude of injected reactive power, Q_{inj} as in (11) and (12). Lastly, the flow pattern as in Fig. 3(d) (which is type 4) implies that instead of supplying reactive power, the line becomes one of the reactive power consumers as the line flows at both ends flowing into it. The suitable representation for this type is a load connected at bus '*k*' as in Fig. 4(b) with extracted reactive power, Q_{ext} as in (13).

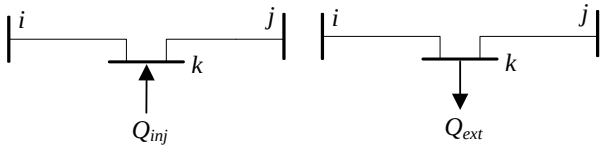

Fig. 4. Modification on transmission line: (a) type 2 & 3 (b) type 4.

$$Q_{inj} = Q_j - Q_i \quad (11)$$

$$Q_{inj} = Q_i + Q_j \quad (12)$$

$$Q_{ext} = Q_i + Q_j \quad (13)$$

3 Blended Crossover Continuous Ant Colony Optimization (BX-CACO)

In this paper, a newly developed hybrid ant colony algorithm is proposed, which is called as Blended Crossover Continuous Ant Colony Optimization (BX-CACO). The newness proposed in the hybrid algorithm is about the hybrid mean, which is calculated during solution update process. Adoption with crossover operator of Genetic Algorithm (GA) is to produce wide variety of solution so as to prevent pre-mature convergence problem as what happens in the original algorithm.

3.1 Ant Colony Optimization for Continuous Domain (ACO_R)

In fact, the proposed BX-CACO was inspired by the original algorithm, which is termed as continuous domain Ant Colony Optimization (ACO_R) as proposed by K. Socha in 2008. Much earlier than Socha's ACO_R, there is another ant colony algorithm which was proposed by M. Dorigo in 1992, known as traditional or original Ant Colony Optimization (ACO) and is the father of all recent ACO algorithms. The uniqueness and attractiveness of ACO is about fast convergence property. Even only small population is utilized, this algorithm is able to provide optimal solution within only small computation time. Such powerful property has motivated this research to implement the ant colony technique.

However, not all problems can be formulated using traditional ACO as there is a need to specify the fitness between two ant's nodes prior to implement it. Only the problems like finding the combination that will result to the best fitness are suitable such as the shortest path, time, and cost, in which all the objectives are already specified between two ant's nodes. For the problems like tuning and sizing, traditional ACO is not recommended because the algorithm will perform the optimization like a trial-and-error approach. To counter this weakness, ACO_R has been proposed for continuous domain optimization (such as tuning and sizing problem) without changing the original working flow as in the traditional one. In ACO_R, the *Solution Archive-T* (a table where each ant stores their updated solutions) is introduced, as illustrated in Fig. 5. The new solution is produced by means of Gaussian normal sampling as in (14), in which the required mean and standard deviation for the sampling is given in (15).

$$S^c_{new,m} = N(S^c_t, \sigma^c_m) \quad (14)$$

$$\sigma^c_m = \xi \sum_{e=1}^{T} \frac{|S^c_e - S^c_t|}{T-1} \quad (15)$$

Where,

$\sigma_m{}^c$: standard deviation of *c*-th control variable of *m*-th ant

S_t^c : mean selected from *t*-th solution of *c*-th control variable in archive *T* by *m*-th ant

$S_e{}^c$: other non-mean solutions of *c*-th control variable in archive *T*

ξ : pheromone evaporation rate

e : *e*-th solutions in archive *T* where $e \neq t$

T : Size of *Archive-T*

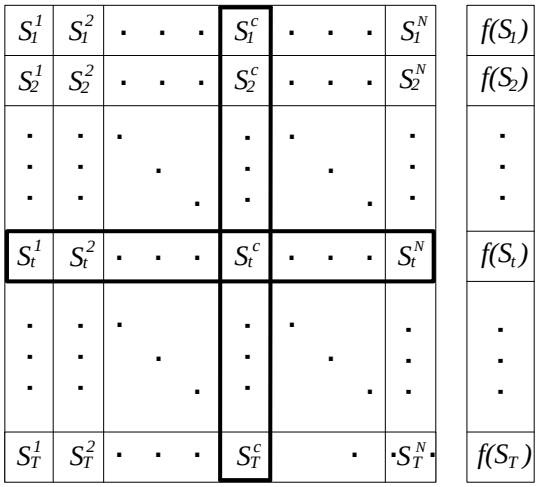

Fig. 5. A *Solution Archive T* contains '*T'* number of chosen solutions stored by the ants after each tour. The solutions are sorted according to their quality of fitness, $f(S_t)$ i.e. the best solution will be placed at the top of the table.

3.2 Hybridization Technique and Algorithm Development

As a matter of fact, the purpose of adopting crossover operator of GA into ACO_R is to improve its intelligence when determining the best solution. Based on experiment, it is found that ACO_R performed well in small test systems. However, it becomes the worst as the size of test system goes larger. This is because of too many control variables have to be tuned and as a result of less solution variety, ACO_R confronts with pre-mature convergence problem, a phenomenon where an algorithm converges too early before the best solution is found. The algorithm of BX-CACO is similar to ACO_R, except during solution update process in which the hybrid mean and standard deviation are calculated in different manner. The proposed algorithm is presented as follows.

Step 1: *Initialization* - First of all, fundamental parameters of BX-CACO such as pheromone evaporation rate, ξ and crossover constant, α are initialized. Low value of ξ will result to fast convergence speed and vice versa, whereas α indicates how much percentage of crossover desired to be used. It should be noted that too fast convergence speed does not necessarily guarantee the quality of fitness. After that, the *Solution Archive-T* is initialized with *T* number of randomly generated solutions.

Step 2: *Fitness Evaluation* - Subsequently, the randomly generated solutions are evaluated by calculating their fitness. Later, the solutions are sorted according to their quality of fitness so that the archive is always in ordered condition.

Step 3: *Solution Update Process* - A modification has been done in BX-CACO for this stage. Unlike ACO_R, BX-CACO applies the concept of exploitation and exploration as proposed in the traditional algorithm. Prior to calculating the hybrid mean, firstly, two parental solutions are chosen based on a randomly generated number, *q* between [0, 1] and a constant, q_0 which is also specified in the same range. If $q < q_0$, the ant prefers exploitation, that is, it will select the best parental solutions in the *Archive-T* which are also the first and second solution from the top. Otherwise, it will perform exploration of solutions, which means that regardless of the quality, the ant will choose the parental solutions randomly from the archive. The next step is to calculate the hybrid mean by '*blending*' two parental solutions together via blended-crossover (BLX-α) operator as in (16) [28] – [29] and simultaneously, the corresponding standard deviation is determined through the modified equation as in (18). Later, the new solution, or also called offspring is generated via normal sampling technique as in (14) using the calculated hybrid mean and standard deviation. For the purpose of this research, Box-Miller technique has been implemented to perform such sampling.

$$\overline{S_m^c} = \begin{cases} (1-\gamma_m^c).S_{t1}^c + \gamma_m^c.S_{t2}^c & \Leftrightarrow \quad S_{t1}^c \le S_{t2}^c \\ (1-\gamma_m^c).S_{t2}^c + \gamma_m^c.S_{t1}^c & \Leftrightarrow \quad S_{t2}^c \le S_{t1}^c \end{cases} \tag{16}$$

$$\gamma_m^c = (1+2\alpha).u - \alpha \tag{17}$$

$$\sigma_m^c = \xi \sum_{t=1}^{T} \frac{|\, S_t^c - \overline{S}_m^c \,|}{T} \tag{18}$$

Where,

$\overline{S}_m^c$: hybrid mean of *c*-th control variable for *m*-th ant
S_{t1}^c, S_{t2}^c : selected parents for crossover
S_t^c : other *t*-th solutions in the archive
γ_m^c : crossover operator
α : crossover constant
u : random number generated within [0, 1]

Step 4: *Fitness Evaluation of Offspring* - The fitness of a new solution generated by each ant is calculated after they have completed the tour.

Step 5: *Updating the Solution Archive T* - At this stage, the existing solutions (parental solutions) in the archive are combined together with the new solutions (offspring) and sorted according to their

fitness quality. To maintain the size of the archive, only *T* number of solutions are deserved to remain. So, the other *m* number of solutions from the bottom are rejected.

Step 6: *Convergence Test* - The algorithm will execute the task from step 3 to 5 until the achievement of convergence, that is, when all solutions in the archive have tolerable difference of fitness.

Fig. 6 gives the illustrative representation of BX-CACO's working flow. Its performance has been justified and validated in [30] – [31].

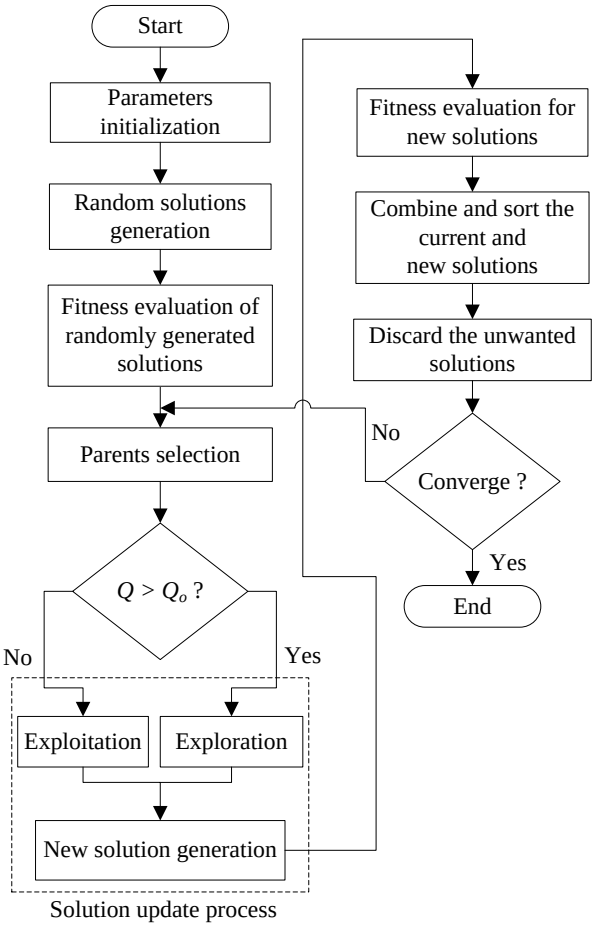

Fig. 6: Full algorithm for implementing BX-CACO based load tracing

4 Formulation Technique

Implementing power tracing via optimization enables a system operator (SO) to trace the power in any system's conditions. As the matrix inversion is not required, possibility of matrix to be singular is not exist and thus, enhancing the advantage of utilizing optimization technique. Such benefit has motivated this research to implement optimization algorithm instead of conventional matrix operation as what previous methods did.

Optimization assisted power tracing is considered to be a new approach, especially when implementing via Artificial Intelligence (AI) optimization. As there are many control variables and constraints have to be considered during formulation task, such approach is rarely applied by researchers. Furthermore, formulating power tracing via optimization is very difficult since an objective function ought to be derived in accordance to the formulated problem. Failure to develop an effective algorithm and appropriate objective function will result to computational burden during optimization, especially for large scale system. However, if a good formulation technique has been established by a designer, all the complexities can be solved. The proposed formulation technique is as follows.

i) Control variables - For simplicity, all the control variables are placed in a large matrix, **X** as in (19), which also represents a *t*-th individual in *Archive-T*.

$$\mathbf{X} = \begin{bmatrix} x_{r1}^{1} & \cdots & x_{r1}^{i} & \cdots & x_{r1}^{nload} \\ x_{r2}^{1} & & x_{r2}^{i} & & x_{r2}^{nload} \\ \vdots & \ddots & \vdots & \ddots & \vdots \\ x_{rl}^{1} & & x_{rl}^{i} & & x_{rl}^{nload} \\ \vdots & & \vdots & & \vdots \\ x_{r,nbr}^{1} & \cdots & x_{r,nbr}^{i} & \cdots & x_{r,nbr}^{nload} \\ x_{g1}^{1} & & x_{g1}^{i} & & x_{g1}^{nload} \\ x_{g2}^{1} & & x_{g2}^{i} & & x_{g2}^{nload} \\ \vdots & \ddots & \vdots & \ddots & \vdots \\ x_{gk}^{1} & & x_{gk}^{i} & & x_{gk}^{nload} \\ \vdots & & \vdots & & \vdots \\ x_{g,ngen}^{1} & \cdots & x_{g,ngen}^{i} & \cdots & x_{g,ngen}^{nload} \end{bmatrix} \quad (19)$$

The control variables that will be tuned are line flow and generator's power fractions extracted by *i*-th load ($x_{fl}^{\ i}$ and $x_{g}^{\ i}$). The line flow fraction, $x_{fl}^{\ i}$ consists of two parts, which are sending and receiving end fraction ($x_{sl}^{\ i}$ and $x_{rl}^{\ i}$). For the purpose of load tracing, it is more suitable to choose $x_{rl}^{\ i}$ to be the control variable as the receiving end power consumed directly by loads. The size of **X** is (*nbr* + *ngen*) x *nload*, where *nbr*, *ngen*, and *nload* are the number of lines, generators, and loads respectively. In addition, it is important to note that the terms generators and loads are replaced with reactive sources and sinks including all elements discussed in subsection 2.3 provided that reactive power load tracing is to be performed. The sending end and

losses fraction due to *i*-th load can be alternatively determined via (20) [14] and (21) respectively.

$$x_{sl}^{i} = \frac{P_{sl}}{P_{rl}} . x_{rl}^{i} \quad (20)$$

$$x_{loss,l}^{i} = x_{sl}^{i} - x_{rl}^{i} \quad (21)$$

Where P_{sl} and P_{rl} (or Q_{sl} and Q_{rl}) represent the sending and receiving end power of *l*-th line respectively. The reason why (21) has been established because of its ability to speed up the searching mechanism as compared to the method proposed by [32] which representing directly $x_{loss,l}^{i}$ as the control variable in matrix **X**.

ii) Equality and non equality constraints - The equality constraints used for ensuring no violation on power flow results can be represented by (5) and (6) for real and (9) and (10) for reactive power tracing. Meanwhile, the non equality constraints for ensuring no negative sharing among loads (or reactive sinks) are specified as follows [14].

$$x_{sl}^{i}, x_{rl}^{i}, x_{loss,l}^{i}, x_{gk}^{i} \geq 0 \quad (22)$$

$$y_{sl}^{i}, y_{rl}^{i}, y_{loss,l}^{i}, y_{sk}^{i} \geq 0 \quad (23)$$

iii) Objective function - A hypothetical equation has been derived to be utilized as the fitness for guiding the BX-CACO algorithm in searching mechanism. Logically, power consumed by a load (or reactive sink) should be equal to the total extracted generator's power minus with the total losses due to that load, or mathematically:

$$P_{Li} = \sum_{k=1}^{ngen} P_{gk}^{i} - \sum_{l=1}^{nbr} P_{loss,l}^{i} \quad (24)$$

The loss of *l*-th line due to a load is described by (25).

$$P_{loss,l}^{i} = x_{loss,l}^{i} . P_{Li} \quad (25)$$

By substituting (2) and (25) into (24), the following is obtained.

$$P_{Li} = \sum_{k=1}^{ngen} x_{gk}^{i} . P_{Li} - \sum_{l=1}^{nbr} x_{loss,l}^{i} . P_{Li} \quad (26)$$

After simplification:

$$1 = \sum_{k=1}^{ngen} x_{gk}^{i} - \sum_{l=1}^{nbr} x_{loss,l}^{i} \quad (27)$$

Rearrange (27):

$$\sum_{k=1}^{ngen} x_{gk}^{i} - \sum_{l=1}^{nbr} x_{loss,l}^{i} - 1 = 0 \quad (28)$$

Or:

$$E_{Li}(x) = \sum_{k=1}^{ngen} x_{gk}^{i} - \sum_{l=1}^{nbr} x_{loss,l}^{i} - 1 = 0 \quad (29)$$

$$\therefore \min\left\{ E_{Li}(x) = \sum_{k=1}^{ngen} x_{gk}^{i} - \sum_{l=1}^{nbr} x_{loss,l}^{i} - 1 \right\} \quad (30)$$

The fitness in (30) will be applied in BX-CACO search engine to provide a finite searching guideline when manipulating the control variables in matrix **X**. The objective of BX-CACO is to minimize the individual generation-demand balance error, E_{Li} as low as possible. For reactive power tracing, simply replace the '*x*' terms in (30) with '*y*'.

As can be observed, all constraints and objective function are linear, which means that instead of applying meta-heuristic optimization, other linear programming (LP) solvers can also be alternative. However after conducting study on such method, it is found that formulating power tracing via LP is not very effective as it requires additional variables to be introduced, such as slack and artificial variables [33]. This will contribute to computational burden since power tracing has already too many control variables to be considered even without such additional variables. Moreover, LP is not very user-friendly as compared to meta-heuristic optimization since its formulation technique is complicated to be implemented, especially when utilizing simplex method based LP that requires complex matrix operation. This is the main reason why this research prefers to implement AI based optimization.

5 Results and Discussion

Validation on IEEE 30-bus reliability test system (RTS) has been performed together with comparative studies. Instead of real power tracing, this paper intends to discuss about reactive power tracing in justifying the performance and reliability of the proposed method. This is because reactive power tracing is more complicated as too many

control variables are involved and various considerations have to be taken into account during formulation task. Besides that, the analysis also involves other conventional methods such as Topological Load Distribution Factor (TLDF) and Bus Impedance Matrix (BIM) technique as proposed in [9] and [10] respectively. After evaluating the performance, comparative study between various AI optimizations are carried out to observe the capability of BX-CACO in terms of computation speed and solution quality.

5.1 Allocation of reactive sources power to reactive sinks

Allocation of reactive sources power to reactive sinks means that a task to trace the reactive sources power extracted by individual reactive sink (including generators, loads and all considerations in subsection 2.3). Table 1, 2, and 3 tabulates the results for BX-CACO, TLDF, and BIM respectively. Obviously, BX-CACO and TLDF result to identical number of reactive sources and sinks. As can be seen, there are fourteen reactive sources (six generators, two capacitors, and six type 2 and 3 lines) and twenty four reactive sinks (twenty one loads and three type 4 lines). Contrary to both methods, BIM provides different results as there are only eight reactive sources (excluding type 2 and 3 lines) and twenty one reactive sinks (excluding type 4 lines). From this point, it is said that BIM has different viewpoint on the terms 'reactive sources' and 'reactive sinks', that is, only the generators and other shunt equipments such as capacitor banks are responsible for supplying reactive power, whereas only the loads consume the supplied power. The line flow patterns as discussed in previous section are not considered by the method, and thus resulting to unreliable reactive power allocation.

In addition, the values of traced powers are also different for all methods. For instance, the reactive power of generator G2 extracted by load L2 are 8.741, 12.670, and 1.806 MVar for BX-CACO, TLDF, and BIM respectively. As a result, the total

Table 1
MVar Sources Allocation to Reactive Sinks via BX-CACO

Reactive Sources	Reactive Sinks												
	L2	L3	L4	L5	L7	L8	L10	L12	L14	L15	L16	L17	L18
G1	0.000	0.011	0.000	0.000	0.000	0.000	0.000	0.000	0.000	0.000	0.000	0.000	0.000
G2	8.741	0.008	1.129	0.000	0.000	0.000	0.000	0.687	0.120	0.240	0.169	1.223	0.289
G5	0.559	0.001	0.539	18.962	10.921	0.000	0.000	2.997	0.068	0.006	0.021	0.014	0.008
G8	2.277	0.001	0.006	0.000	0.000	29.948	0.000	0.000	0.740	0.819	0.409	3.256	0.562
G11	0.921	1.336	0.055	0.000	0.000	0.000	0.662	0.064	0.068	0.212	0.071	0.712	0.052
G13	0.000	0.000	0.000	0.000	0.000	0.000	0.000	4.577	0.826	1.857	1.230	0.343	0.022
C10	0.000	0.000	0.000	0.000	0.000	0.000	1.377	0.000	0.000	0.000	0.000	3.106	0.000
C24	0.000	0.000	0.000	0.000	0.000	0.000	0.000	0.000	0.000	0.000	0.000	0.000	0.000
ℓ3	0.000	0.000	0.045	0.000	0.000	0.000	0.000	0.078	0.014	0.020	0.002	0.023	0.049
ℓ8	0.002	0.987	0.032	0.000	0.000	0.000	0.000	0.009	0.040	0.004	0.060	0.031	0.001
ℓ9	0.099	0.000	0.005	0.000	0.000	0.000	0.000	0.135	0.002	0.035	0.024	0.010	0.001
ℓ10	0.089	0.010	0.001	0.000	0.000	0.000	0.000	0.001	0.036	0.020	0.000	0.009	0.055
ℓ40	0.000	0.000	0.000	0.000	0.000	0.000	0.000	0.000	0.000	0.000	0.000	0.000	0.000
ℓ41	0.000	0.000	0.000	0.000	0.000	0.000	0.000	0.000	0.000	0.000	0.000	0.000	0.000
Total	12.688	2.355	1.811	18.962	10.922	29.948	2.039	8.548	1.915	3.213	1.986	8.726	1.038

Reactive Sources	Reactive Sinks											Total Sources
	L19	L20	L21	L23	L24	L26	L29	L30	ℓ4	ℓ5	ℓ12	
G1	0.000	0.000	0.000	0.000	0.000	0.000	0.000	0.000	5.151	0.000	0.000	5.163
G2	3.054	0.000	0.000	0.420	0.007	0.058	0.105	0.178	13.211	2.203	0.000	31.841
G5	0.006	0.000	0.000	0.258	0.002	0.002	0.169	0.003	0.003	2.123	0.660	37.321
G8	0.006	0.000	0.000	0.484	0.117	0.039	0.005	0.002	0.000	0.601	0.064	39.338
G11	0.002	0.000	12.365	0.185	0.078	0.012	0.150	0.195	0.087	3.580	0.351	21.157
G13	0.086	0.000	0.000	0.177	1.908	0.072	0.001	5.297	0.000	0.000	0.000	16.397
C10	0.498	0.910	0.001	0.000	5.040	2.690	0.269	4.816	0.000	0.000	0.293	19.000
C24	0.000	0.000	0.000	0.000	0.005	0.032	0.013	4.250	0.000	0.000	0.000	4.300
ℓ3	0.000	0.000	0.000	0.010	0.039	0.001	0.001	0.001	0.019	0.000	0.000	0.304
ℓ8	0.017	0.000	0.000	0.037	0.008	0.053	0.000	0.029	0.037	0.219	0.051	1.619
ℓ9	0.038	0.000	0.000	0.020	0.050	0.015	0.017	0.017	0.001	0.069	0.006	0.544
ℓ10	0.003	0.000	0.000	0.026	0.115	0.003	0.000	0.016	0.002	0.128	0.002	0.515
ℓ40	0.000	0.000	0.000	0.000	0.000	0.000	0.390	3.826	0.000	0.000	0.000	4.216
ℓ41	0.000	0.000	0.000	0.000	0.000	0.000	1.842	10.848	0.000	0.000	0.000	12.690
Total	3.710	0.911	12.366	1.618	7.369	2.977	2.964	29.479	18.512	8.923	1.426	194.407

Note: The symbols G, L, l, and C represent the generator bus, load bus, line number, and capacitor bus respectively.

reactive sources powers (at the bottom and right most of each table) are also different in which 194.407 MVar for BX-CACO, 155.755 MVar for TLDF, and 174.518 MVar for BIM. However, such different values do not necessarily mean that there must be an error among the three methods. It is because of their different point of views when performing electricity tracing.

Firstly, the proposed technique performs power flow results based tracing, that is, all the parameters from power flow results (such as generator's and load's power, line flow, and losses) are not modified and used directly in the tracing algorithm. To be more precise, there is no need to modify the condition of power system and it is used in the proposed algorithm as it is. On the contrary, TLDF requires the system to be treated as lossless and to achieve this, the concept of net flow is utilized. In the concept, all transmission lines have lossless flows and the line losses are compensated by means of subtracting from each generator's power to obtain net generation. This implies that all generators will have generated powers that have been subtracted with their contributed losses. Such modification on power system becomes the main reason why its results contradict with the proposed technique. Moreover, another reason that makes TLDF disagrees with BX-CACO is because of the need to implement Proportional Sharing Principle (PSP), which is not required in the proposed algorithm. Lastly, BIM performs electricity tracing based on circuit theory approach. It begins with Ohm's Law to obtain the traced voltages, and subsequently multiplies with traced currents to determine the traced complex powers. Unfortunately, such approach results to negative participation of loads, for example in Table 3 there are twelve loads (L2 – L5, L7, L10, L14, L15, L18 – L20, L29) have negative sharing on generator G1. In transmission service pricing viewpoint, negative sharing is not acceptable as this will result to negative allocated charge, which means that instead of paying to service provider, such consumer gains benefit as a result of the provided services.

Table 2
MVar Sources Allocation to Reactive Sinks via TLDF

Reactive	Reactive Sinks												
Sources	L2	L3	L4	L5	L7	L8	L10	L12	L14	L15	L16	L17	L18
G1	0.000	0.642	0.000	0.000	0.000	0.000	0.000	0.000	0.000	0.000	0.000	0.000	0.000
G2	12.670	0.556	0.249	0.000	0.000	0.000	0.000	0.404	0.086	0.135	0.097	0.132	0.048
G5	0.003	0.000	0.129	19.000	9.545	0.000	0.000	0.209	0.045	0.070	0.050	0.068	0.025
G8	0.012	0.001	0.522	0.000	0.000	30.000	0.000	0.846	0.181	0.282	0.203	0.277	0.102
G11	0.013	0.001	0.577	0.000	0.000	0.000	0.657	0.936	0.200	0.312	0.225	1.405	0.112
G13	0.000	0.000	0.000	0.000	0.000	0.000	0.000	4.906	1.047	1.635	1.177	1.605	0.589
C10	0.000	0.000	0.000	0.000	0.000	0.000	1.343	0.000	0.000	0.000	0.000	2.247	0.000
C24	0.000	0.000	0.000	0.000	0.000	0.000	0.000	0.000	0.000	0.000	0.000	0.000	0.000
ℓ3	0.000	0.000	0.031	0.000	0.000	0.000	0.000	0.051	0.011	0.017	0.012	0.017	0.006
ℓ8	0.000	0.000	0.018	0.000	1.355	0.000	0.000	0.030	0.006	0.010	0.007	0.010	0.004
ℓ9	0.001	0.000	0.038	0.000	0.000	0.000	0.000	0.061	0.013	0.020	0.015	0.020	0.007
ℓ10	0.001	0.000	0.036	0.000	0.000	0.000	0.000	0.058	0.012	0.019	0.014	0.019	0.007
ℓ40	0.000	0.000	0.000	0.000	0.000	0.000	0.000	0.000	0.000	0.000	0.000	0.000	0.000
ℓ41	0.000	0.000	0.000	0.000	0.000	0.000	0.000	0.000	0.000	0.000	0.000	0.000	0.000
Total	12.700	1.200	1.600	19.000	10.900	30.000	2.000	7.500	1.600	2.500	1.800	5.800	0.900

Reactive	Reactive Sinks											Total
Sources	L19	L20	L21	L23	L24	L26	L29	L30	ℓ4	ℓ5	ℓ12	Sources
G1	0.000	0.000	0.000	0.000	0.000	0.000	0.000	0.000	0.510	0.000	0.000	1.152
G2	0.053	0.000	0.000	0.086	0.094	0.032	0.003	0.072	0.517	1.682	0.000	16.916
G5	0.027	0.000	0.000	0.045	0.048	0.017	0.006	0.140	0.039	6.919	0.092	36.477
G8	0.110	0.000	0.000	0.181	0.196	0.067	0.086	1.901	0.158	0.002	0.374	35.500
G11	0.918	0.230	3.678	0.200	1.239	0.425	0.064	1.415	0.175	0.002	0.568	13.351
G13	0.639	0.000	0.000	1.047	1.137	0.390	0.039	0.877	0.000	0.000	0.000	15.088
C10	1.627	0.470	7.522	0.000	2.089	0.717	0.073	1.611	0.000	0.000	0.315	18.015
C24	0.000	0.000	0.000	0.000	1.850	0.635	0.064	1.426	0.000	0.000	0.000	3.976
ℓ3	0.007	0.000	0.000	0.011	0.012	0.004	0.000	0.009	0.009	0.000	0.000	0.196
ℓ8	0.004	0.000	0.000	0.006	0.007	0.002	0.001	0.020	0.006	0.000	0.013	1.499
ℓ9	0.008	0.000	0.000	0.013	0.014	0.005	0.002	0.041	0.011	0.000	0.027	0.297
ℓ10	0.008	0.000	0.000	0.012	0.013	0.005	0.002	0.039	0.011	0.000	0.026	0.281
ℓ40	0.000	0.000	0.000	0.000	0.000	0.000	0.140	3.104	0.000	0.000	0.000	3.244
ℓ41	0.000	0.000	0.000	0.000	0.000	0.000	0.420	9.344	0.000	0.000	0.000	9.764
Total	3.400	0.700	11.200	1.600	6.700	2.300	0.900	20.000	1.436	8.604	1.415	155.755

Note: The symbols G, L, l, and C represent the generator bus, load bus, line number, and capacitor bus respectively.

Table 3
MVar Sources Allocation to Loads via BIM

Reactive Sources	Load Bus										
	L2	L3	L4	L5	L7	L8	L10	L12	L14	L15	L16
G1	-1.990	-0.235	-1.995	-19.707	-0.636	10.071	-0.464	1.706	-0.905	-0.895	0.164
G2	1.806	0.199	0.357	5.773	2.309	5.464	0.538	1.574	0.487	0.713	0.417
G5	2.741	0.306	0.827	9.102	2.773	5.021	0.762	1.692	0.786	1.070	0.499
G8	3.001	0.318	0.869	11.677	3.088	4.253	0.767	1.678	0.805	1.088	0.497
G11	1.631	0.172	0.467	6.328	1.701	2.706	0.372	0.872	0.426	0.568	0.249
G13	1.259	0.131	0.354	4.914	1.340	2.171	0.316	0.508	0.283	0.391	0.177
C10	1.479	0.156	0.421	5.726	1.554	2.504	0.321	0.778	0.384	0.508	0.219
C24	0.346	0.037	0.098	1.338	0.365	0.589	0.081	0.177	0.087	0.112	0.052
Total	10.274	1.085	1.399	25.150	12.494	32.779	2.693	8.985	2.354	3.555	2.273

Reactive Sources	Load Bus										Total Sources
	L17	L18	L19	L20	L21	L23	L24	L26	L29	L30	
G1	1.392	-0.380	-0.524	-0.196	2.778	0.162	2.381	0.639	-0.169	13.965	5.163
G2	1.278	0.274	0.942	0.202	2.513	0.390	1.473	0.543	0.261	4.330	31.841
G5	1.361	0.417	1.287	0.291	2.663	0.464	1.426	0.567	0.359	2.907	37.321
G8	1.336	0.424	1.295	0.294	2.608	0.462	1.379	0.548	0.354	2.599	39.338
G11	0.631	0.216	0.645	0.146	1.219	0.235	0.674	0.289	0.196	1.413	21.157
G13	0.514	0.161	0.499	0.116	1.041	0.168	0.529	0.229	0.155	1.141	16.397
C10	0.535	0.192	0.564	0.128	1.028	0.207	0.580	0.259	0.178	1.278	19.000
C24	0.136	0.044	0.134	0.031	0.245	0.039	0.073	0.046	0.038	0.233	4.300
Total	7.183	1.349	4.842	1.011	14.094	2.126	8.516	3.121	1.372	27.866	174.518

Note: The symbols G, L, l, and C represent the generator bus, load bus, line number, and capacitor bus respectively.

Mathematically, if the total reactive sources power of TLDF is summed with total reactive losses, the result will be identical to that of BX-CACO, that is 155.755 + 38.652 = 194.407 MVar. This is similar for BIM if its total reactive sources power is summed with total reactive power supported by type 2 and 3 lines (line 3, 8, 9, 10, 40, 41), which is 174.518 + 0.304 + 1.619 + 0.544 + 0.515 + 4.216 + 12.690 = 194.407 MVar. This calculation has proven that there is no error in all methods except different point of views when formulating the tracing algorithm.

5.2 Algorithm Performance

The capability of BX-CACO in performing optimization is analyzed in terms of computation speed and solution optimality. Comparative study involving various AI optimizations such as the original ACO_R, Evolutionary Programming (EP), and Genetic Algorithm (GA) are carried out on four test systems, which are IEEE 14-bus, 26-bus, 30-bus, and 57-bus RTS as tabulated in Table 4. The convergence graphs of 57-bus system for all algorithms within 360 minutes are illustrated in Fig. 7. For the purpose of this research, the value of ξ and α are 0.95 and 0.01 respectively.

First of all, it is discovered that BX-CACO and ACO_R perform the fastest optimization process for the first three systems where at most 30 minutes is required for convergence. For 57-bus system, there is a significant difference between both algorithms where the resulted computation time is 145 minutes for BX-CACO, which is 35 minutes earlier than ACO_R. However, the resulted computation time by EP and GA has larger difference especially for 30-bus and 57-bus system, where both of them finish the optimization about 90 minutes after the ant colony algorithms. Such significant difference is due to required population size, where only 5 individuals are required by ant colony approaches as compared to EP and GA which require 50 individuals in the population.

Table 4
Performance Comparison on Various Algorithms

Test Systems	Algorithms	E_{Li}	t_c (minutes)	PS
14-Bus	BX-CACO	3.5×10^{-5}	3	5
	ACO_R	6.6×10^{-4}	12	5
	EP	5.0×10^{-5}	13	50
	GA	3.3×10^{-2}	12	50
26-Bus	BX-CACO	2.4×10^{-3}	20	5
	ACO_R	3.3×10^{-3}	20	5
	EP	2.3×10^{-3}	35	50
	GA	1.8×10^{-1}	60	50
30-Bus	BX-CACO	2.0×10^{-3}	25	5
	ACO_R	3.3×10^{-2}	30	5
	EP	2.6×10^{-3}	120	50
	GA	4.6×10^{-1}	120	50
57-Bus	BX-CACO	2.0×10^{-2}	145	5
	ACO_R	1.4×10^{-1}	180	5
	EP	1.0×10^{-2}	240	50
	GA	5.7×10^{-1}	240	50

E_{Li}, t_c, and PS are the optimal objective function, computation time, and population size respectively.

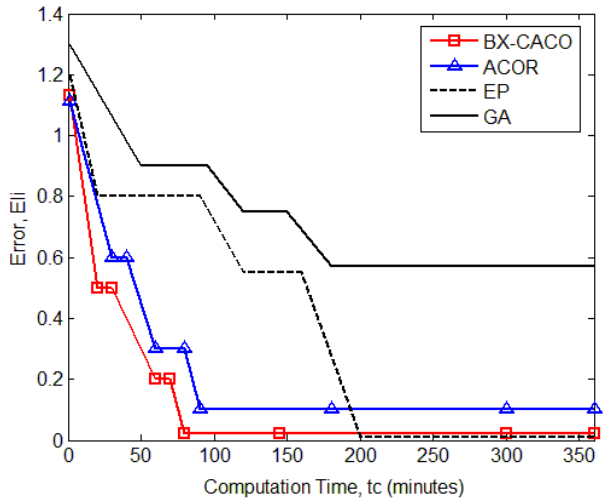

Fig. 7. Convergence graphs for all algorithms

Secondly, it is seen that BX-CACO and EP result to comparable fitness for all test systems. In average, the resulted errors, E_{Li} by both methods are 4.25 x 10^{-5}, 2.35 x 10^{-3}, 2.3 x 10^{-3}, and 1.5 x 10^{-2} for 14-bus, 26-bus, 30-bus, and 57-bus system respectively. Such comparable results justify the capability of BX-CACO in providing reliable solutions regardless of system sizes. As compared to this hybrid algorithm, ACO_R performs well only for the first three systems, which are 14-bus to 30-bus system. Unfortunately, it fails to reduce E_{Li} towards zero for 57-bus system as the resulted fitness is still considerably high, which is 0.14 and this is called as pre-mature convergence of ACO_R when large scale system is used. As can be observed in Fig. 7, ACO_R starts to converge at about 90 minutes of computation time before fully converged at 180 minutes, where the resulted fitness is still high and much above than BX-CACO and EP. This is the main reason for adopting crossover operator of GA into the original algorithm, that is, to create a more intelligent algorithm when searching the best solution while maintaining the fast convergence property concurrently. The '*blending*' concept applied for producing hybrid mean has improved the ability of BX-CACO in providing wide solution variety, thus enhancing its intelligence when updating the solution. The worst performance is only provided by GA where only 14-bus system can be used. The rest systems are not suggested as the resulted E_{Li} values are above than 0.05, which is the maximum tolerable value of fitness.

In overall, inspection from Fig. 7 has justified that ant colony algorithms being the fastest technique, however the quality of E_{Li} resulted by original algorithm is not as good as the hybrid one. Although EP results to comparable fitness as BX-CACO, the required computation time for convergence is too long. Lastly, GA reflects the worst performance as it fails to provide further reduction of error even after 360 minutes.

6 Conclusion

In conclusion, an optimization assisted power tracing has been proposed by incorporating a hybrid algorithm as an engine to perform tracing process. Contrary to previous methods that are based on matrix operation and rely on assumption like PSP, the proposed technique tries an alternative approach. With simple formulation steps, free from matrix singularity dependency, as well as any assumptions, BX-CACO assisted power tracing has reflected capable performance for real system applications in deregulated environment. Moreover, by implementing the hybrid algorithm for electricity tracing, computational burden problem as what happened in population based algorithms is successfully solved as it is able to find the best solution within acceptable computation time regardless of system sizes. For future recommendation, it is aspired that the proposed power tracing algorithm is not only implemented in the field of transmission service pricing, but also in other fields concerning voltage stability improvement.

Acknowledgement

The authors would like to acknowledge The Research Management Institute (RMI) UiTM, Shah Alam and Ministry of Higher Education Malaysia (MOHE) for the financial support of this research. This research is jointly supported by Research Management Institute (RMI) via the Excellence Research Grant Scheme UiTM with project code: 600-RMI/ST/DANA 5/3/Dst (164/2011) and MOHE under the Exploratory Research Grant Scheme (ERGS) with project code: 600-RMI/ERGS 5/3 (14/2011).

References:

[1] Z. Ming, S. Liying, L. Gengyin, Y. Ni, A Novel Power Flow Tracing Approach Considering Power Losses, *Proceedings of the IEEE International Conference on Electric Utility Deregulation, Restructuring and Power Technologies* (DRPT), Vol.1, 2004, pp. 355 – 359.

[2] M. Pantos, F. Gubina, Ex-ante Transmission Service Pricing via Power Flow Tracing,

Electrical Power and Energy System, Vol. 26, 2004, pp. 509 – 518.

[3] P. Barcia, R. Pestana, Tracing the Flows of Electricity, *Electrical Power and Energy Systems*, Vol. 32, 2010, pp. 329 – 332.

[4] M. S. S. Rao, S. A. Soman, P. Chitkara, R. K. Gajbhiye, N. Hemachandr, B. L. Menezes, Min-Max Fair Power Flow Tracing for Transmission System Usage Cost Allocation: A Large System Perspective, *IEEE Transactions on Power Systems*, Vol. 25, 2010, pp. 1457 – 1468.

[5] Y. C. Chang, C. N. Lu, An Electricity Tracing Method with Application to Power Loss Allocation, *Electrical Power and Energy Systems*, Vol. 23, 2001, pp. 13 – 17.

[6] P. Nallagownden, R. N. Mukerjee, S. Masri, Power Tracing and Prediction of Losses for Deregulated Transmission System, *International Journal of Electrical & Computer Sciences*, Vol. 10, 2010, pp. 97 – 103.

[7] K. Xiea, J. Zhoua, W. Li, Analytical Model and Algorithm for Tracing Active Power Flow Based on Extended Incidence Matrix, *Electric Power Systems Research*, Vol. 79, 2009, pp. 399 – 405.

[8] J. Bialek, Topological Generation and Load Distribution Factors for Supplement Charge Allocation in Transmission Open Access, *IEEE Transactions on Power Systems*, Vol. 12, 1997, pp. 1185 – 1193.

[9] J. Bialek, Tracing The Flow of Electricity, *Generation, Transmission and Distribution, IEE Proceedings*, Vol. 143, 1996, pp. 313 – 320.

[10] J. H. Teng, Power Flow and Loss Allocation for Deregulated Transmission Systems, *Electrical Power and Energy Systems*, Vol. 27, 2005, pp. 327 – 333.

[11] P. Wei, Y. Ni, F. F. Wu, Load Flow Tracing in Power Systems with Circulating Power, *Electrical Power and Energy Systems*, Vol. 24, 2002, pp. 807 – 813.

[12] P. Wei, B. Yuan, Y. Ni, F. F. Wu, Power Flow Tracing for Transmission Open Access, *International Conference on Electric Utility Deregulation and Restructuring and Power Technologies* (DRPT), 2000, pp. 476 – 481.

[13] S. M. Abdelkader, Complex Power Flow Tracing For Transmission Loss Allocation Considering Loop Flows, *IEEE Power & Energy Society General Meeting* (PES), 2009, pp. 1 – 9.

[14] A. R. Abhyankar, S. A. Soman, and S. A. Khaparde, Optimization Approach to Real Power Tracing: An Application to Transmission Fixed Cost Allocation, *IEEE Transactions on Power Systems*, Vol. 21, 2006, pp. 1350 – 1361.

[15] M. H. Sulaiman, M. W. Mustafa, H. Shareef, S. N. A. Khalid, O. Aliman, Real and Reactive Power Flow Allocation in Deregulated Power System Utilizing Genetic-Support Vector Machine Technique, *International Review of Electrical Engineering (IREE)*, Vol. 5, No. 5, 2010, pp. 2199 – 2208.

[16] M. H. Sulaiman, M. W. Mustafa, H. Shareef, S. N. A. Khalid, An Application of Artificial Bee Colony Algorithm with Least Squares Support Vector Machine for Real and Reactive Power Tracing in Deregulated Power System, *International Journal of Electrical Power and Energy Systems* , Vol. 37, 2012, pp. 67 – 77.

[17] M. Dorigo, *Optimization, Learning and Natural Algorithms*, Ph.D Thesis, Dipartimento, Politecnico di Milano, Italy, 1992.

[18] M. Dorigo, T. Stutzle, *Ant Colony Optimization*, Massachusetts Institute of Technology, 2004.

[19] V. Aristidis, An Ant Colony Optimization (ACO) Algorithm Solution to Economic Load Dispatch (ELD) Problem, *WSEAS Transactions on Systems*, Vol. 5, No. 8, 2006, pp. 1763 – 1770.

[20] J. Nikoukar, M. Gandomkar, Capacitor Placement in Distribution Networks Using Ant Colony Algorithm, *WSEAS Transactions on Systems*, Vol. 4, No. 1, 2005, pp. 38 – 42.

[21] C. F. Juang, C. M. Lu, C. Lo, and C. Y. Wang, Ant Colony Optimization Algorithm for Fuzzy Controller Design and Its FPGA Implementation, *IEEE Transactions on Industrial Electronics*, Vol. 55, 2008, pp. 1453 – 1462.

[22] C. F. Juang and C. H. Hsu, Reinforcement Interval Type-2 Fuzzy Controller Design by Online Rule Generation and Q-Value-Aided Ant Colony Optimization, *IEEE Transactions on Systems, Man, and Cybernetics, Part B: Cybernetics*, Vol. 39, 2009, pp. 1528 – 1542.

[23] M. Craus, C. Bulancea, An Improved Load Balance Strategy Using ACO Meta-heuristics, *WSEAS Transactions on Computers*, Vol. 4, No. 8, 2005, pp. 960 – 965.

[24] C. F. Juang and C. H. Hsu, Reinforcement Ant Optimized Fuzzy Controller for Mobile-Robot Wall-Following Control, *IEEE Transactions on Industrial Electronics*, Vol. 56, 2009, pp. 3931 – 3940.

[25] K. Saleem, N. Fisal, M. A. Baharudin, A. A. Ahmed, S. Hafizah, S. Kamilah, Ant Colony Inspired Self-Optimized Routing Protocol Based on Cross Layer Architecture for Wireless Sensor Networks, *WSEAS Transactions on Communications*, Vol. 9, No. 10, 2010, pp. 669 – 678.

[26] K. Socha and M. Dorigo, Ant Colony Optimization for Continuous Domains, *European Journal of Operational Research*, Vol. 185, 2008, pp. 1155 – 1173.

[27] Z. Hamid, I. Musirin, M. M. Othman, M. N. A. Rahim, New Formulation Technique for Generation Tracing via Evolutionary Programming, *International Review of Electrical Engineering (IREE)*, Vol. 6, 2011, pp. 1946 – 1959.

[28] S. S. Reddy, M. S. Kumari, M. Sydulu, Congestion Management in Deregulated Power System by Optimal Choice and Allocation of FACTS Controllers Using Multi-Objective Genetic Algorithm, *The IEEE PES Transmission and Distribution Conference and Exposition*, 2010, pp. 1 – 7.

[29] K. Deb, *Multi-Objective Optimization using Evolutionary Algorithms*, John Wiley and Sons, 2001.

[30] Z. Hamid, I. Musirin, M. N. A. Rahim, Blended Crossover Continuous Ant Colony Optimization and Stability Index Tracing for Effective FACTS Devices Installation, *International Review of Electrical Engineering (IREE)*, Vol. 7, No. 1, 2012.

[31] Z. Hamid, I. Musirin, M. M. Othman, M. N. A. Rahim, Efficient Power Scheduling via Stability Index Based Tracing Technique and Blended Crossover Continuous Ant Colony Optimization, *Australian Journal of Basic and Applied Sciences (AJBAS)*, Vol. 5, No. 9, 2011, pp. 1335 – 1347.

[32] M. H. Sulaiman, M. W. Mustafa, O. Aliman, Transmission Loss and Load Flow Allocations via Genetic Algorithm Technique, IEEE Region 10 Conference (TENCON), 2009, pp. 1 – 5.

[33] J. A. Momoh, *Electric Power System Applications of Optimization*, CRC Press HQ Marcel Dekker, 2001.

Bibliographies

Zulkiffli Abdul Hamid was born in Kedah, Malaysia in 1986. He obtained Diploma in Electrical Engineering (Electronics) in 2007 and Bachelor in Electrical Engineering (Hons) in 2010 from Universiti Teknologi MARA, Malaysia. His research interest includes sizing FACTS devices, Artificial Intelligence (AI) base optimization technique, power tracing and voltage stability field. Currently he is pursuing his Ph.D in power tracing field at the same university.

Ismail Musirin obtained Diploma of Electrical Power Engineering in 1987, Bachelor of Electrical Engineering (Hons) in 1990; both from Universiti Teknologi Malaysia, MSc in Pulsed Power Technology in 1992 from University of Strathclyde, United Kingdom and PhD in Electrical Engineering from Universiti Teknologi MARA, Malaysia in 2004. Assoc. Prof. Dr. Ismail Musirin has published 2 books and more than 80 technical papers in the international and national conferences, and also in the international journals. He is a reviewer of IEEE transactions and IET journals. He is also appointed as the permanent reviewer for the World Scientific and Engineering Academy and Society (WSEAS) centered in Greece. His research interest includes power system stability, optimization techniques, distributed generator and artificial intelligence. He is also a member of IEEE, IEEE Power Engineering Society and Artificial Immune System Society (ARTIST).